Carbohydrate Polymers 121 (2015) 355–361

Contents lists available at ScienceDirect

Carbohydrate Polymers

journal homepage: www.elsevier.com/locate/carbpol

Preparation and structural characterization of poly-mannose synthesized by phosphoric acid catalyzation under microwave irradiation

Haisong Wang[a,b], Xiangrong Cheng[a,b], Yonghui Shi[b], Guowei Le[a,b,*]

[a] Key Laboratory of Industrial Biotechnology, Ministry of Education, Jiangnan University, Wuxi 214122, Jiangsu, PR China
[b] State Key Laboratory of Food Science and Technology, School of Food Science and Technology, Jiangnan University, Wuxi 214122, Jiangsu, PR China

ARTICLE INFO

Article history:
Received 30 September 2014
Received in revised form 9 December 2014
Accepted 12 December 2014
Available online 2 January 2015

Chemical compounds studied in this article:
D-mannose (PubChem CID: 18950)
Phosphoric acid (PubChem CID: 1004)
Ethanol (PubChem CID: 702)
Trifluoroacetic acid (PubChem CID: 6422)

Keywords:
Poly-mannose
Microwave irradiation
NMR
Methylation analysis

ABSTRACT

Poly-mannose with molecular weight of 2.457 kDa was synthesized using D-mannose as substrate and phosphoric acid as catalyst under the condition of microwave irradiation for the first time. The optimum reaction conditions were microwave output power of 900 W, temperature 115 °C, proton concentration 2.5 mol/L, and microwave irradiation time 5 min. The actual maximum yield was 91.46%. After purified by Sepherdex G-25 column chromatography, the structural features of poly-mannose were investigated by high-performance anion-exchange chromatography (HPAEC), high-performance gel-permeation chromatography (HPGPC), infrared (IR) spectroscopy, methylation analysis and NMR spectroscopy analysis (^{1}H, ^{13}C, COSY, TOCSY, HMQC, and HMBC). HPAEC analysis showed that the composition of synthetic polysaccharides was D-mannose, its purity was demonstrated by HPGPC as a single symmetrical sharp peak, and additionally IR spectra demonstrated the polymerization of D-mannose. Methylation analysis and NMR spectroscopy revealed that the backbone of poly-mannose consisting of (1 → 3)-linked β-D-Man*p*, (1 → 3)-linked α-D-Man*p*, and (1 → 6)-linked α-D-Man*p* residues, and the main chain were branched at the O-2, O-3, O-4, O-6 position.

1. Introduction

Polysaccharides as biological macromolecules exhibit a variety of distinct physicochemical, physiological, and pharmaceutical properties (Jiang et al., 2013; Li et al., 2014; MíčKoVá, čopíKoVá, & SyNytSyA, 2007). Most polysaccharides are obtained from plants, animals, and microorganisms (Qu, Liu, & Zhang, 2014; Vu, Chen, Crawford, & Ivanova, 2009; Zia, Anjum, Zuber, Mujahid, & Jamil, 2014). However, the preparation methods often involve lots of prophase work, such as material choice, extraction, isolation, purification to obtain target products while polysaccharides yield rates are low. Therefore, a simple, quick and high efficiency polysaccharides synthesis method is desirable.

Previous studies have shown that sugars can be polymerized in the presence of heat and acid (Allingham, 1982; Li, Le, & Shi, 2006a; Manley-Harris & Richards, 1993). In the polymerization of sugars, acid catalyzes the hydroxyl (C-1) of monosaccharide protonation as glycosyl donors and non-protonated sugars as glycosyl acceptors. The glycoside linkages among sugar molecules are rapidly and efficiently constructed under the condition of microwave irradiation which supports the energy of polymerization. An earlier study successfully synthesized oligosaccharides (Li, Le, Cheng, Wang, & Shi, 2006b) and polydextrose (Wang, Shi, & Le, 2014) using D-glucose as reactant and acid as catalyst under the condition of microwave irradiation. Due to its good processing performance and potential health benefits, polydextrose is widely used as low-energy bulking agent in a variety of foods and a partial replacement for fat and starch (Cerna et al., 2003). Former researches demonstrated that the acid catalyzed and microwave mediated method might be used to synthesize other value added carbohydrate polymers. Due to the structure similarity of D-glucose and D-mannose, the reaction of D-glucose polymerization may be applied to D-mannose. Furthermore, polysaccharides containing D-mannose have many special biological functions. A diet supplemented with aloe poly-mannose has been shown to have positive effects on adults diagnosed with Alzheimer's disease (Lewis et al., 2013) whereas mannan from yeast cell-wall has antioxidant and antimutagenic activity (Križková et al., 2006).

* Corresponding author at: State Key Laboratory of Food Science and Technology, School of Food Science and Technology, Jiangnan University, Wuxi 214122, Jiangsu, PR China. Tel.: +86 510 85917789; fax: +86 510 85917789.
E-mail address: lgw@jiangnan.edu.cn (G. Le).

http://dx.doi.org/10.1016/j.carbpol.2014.12.046
0144-8617/

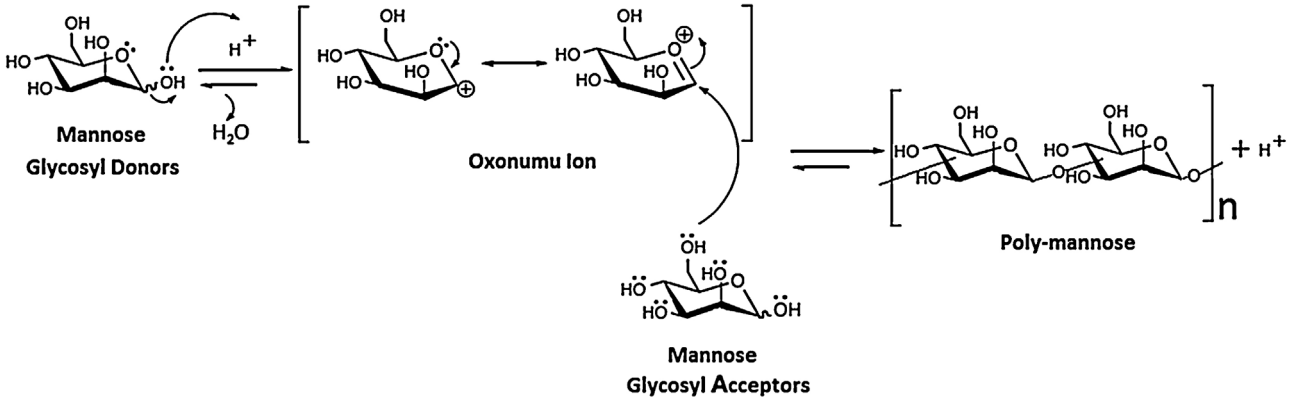

Fig. 1. Synthetic pathway of poly-mannose.

To the best of our knowledge, few studies have investigated rapid and efficient synthesis of poly-mannose by microwave irradiation under the condition of acid catalyzation. To explore new polysaccharides synthesis methods, the aim of the present work was to prepare and characterize the structure of poly-mannose.

2. Materials and methods

2.1. Materials

Deionized and ultrapure water were used. Unless otherwise stated, all chemicals were purchased from Sigma–Aldrich (St. Louis, MO, USA). D-Mannose (AR class) was obtained from Sinopharm Chemical Reagent Co., Ltd. (Shanghai, China). All other chemicals were of analytical grade.

2.2. Preparation of poly-mannose

The poly-mannose was synthesized by acid catalyzation under microwave irradiation according to the method described previously (Wang et al., 2014). Briefly, 50 g D-mannose was added into an open glass container followed by the addition of 6 mL phosphoric acid with proton concentration of 2.5 mol/L and mixed adequately in the glass container. Then the mixture was taken to the cavity of the XH-200A microwave reactor (Beijing Xianghu Science and Technology Development Co., Ltd., Beijing, China) and subjected to microwave irradiation (900 W) at 115 °C for 5 min with constant stirring. When reaction was complete, the mixture was cooled by dry air and crush-up to obtain the crude product (synthetic pathway is shown in Fig. 1.).

2.3. Determination of poly-mannose yield rate

Poly-mannose yield rate was estimated by peak area integration method. The synthetic product was analyzed by HPLC with Sugarpack-1 column under the following conditions: water was used as mobile phase with 0.4 mL/min flow rate, the column oven was kept at 85 °C and the injection volume was 10 μL. The sample was detected with differential refractive index detector (Waters 2410).

2.4. Purification of poly-mannose

The crude product was dissolved in deionized water and then precipitated with five times volume ethanol to obtain D-mannose and acid-free product. The deposition was re-dissolved in deionized water, further concentrated at a temperature of 60 °C under the vacuum of 0.1 MPa, and then lyophilized to obtain white powder. The ethanol precipitated poly-mannose was further purified by gel permeation chromatography of Sephadex G-25 gel column at room temperature. The elution was collected and lyophilized as purified poly-mannose for further analysis.

2.5. Molecular weight determination

Molecular weight of poly-mannose was determined by high-performance size-exclusion chromatography (HPSEC) on a Waters 600 HPLC apparatus equipped with 2410 differential refractive index (RI) detector and Empower workstation (Waters, USA). The analytical column was Ultrahydrogel^{TM} Linear 300 mm × 7.8 mm id × 2. The eluent was $NaNO_2$ (0.1 mol/L) solution containing NaN_3 (0.5 g/L) at a flow rate of 0.9 mL/min. The sample, previously filtered through a membrane (0.22 μm, Millipore), was injected at a concentration of 1 mg/mL. The column oven was kept at 45 °C.

2.6. Monosaccharide composition analysis

Monosaccharide composition of poly-mannose was determined by treating sample (30 mg) in 4 mL of 2 M trifluoroacetic acid (TFA) at 115 °C for 4.5 h. The analysis was carried out using an ICS-5000 high-performance anion-exchange chromatography (HPAEC) (Dionex, USA) according to a previous method (Wang, Liu, Zhou, & Hu, 2012).

2.7. Fourier transform infrared (FT-IR) spectra

The Fourier transform infrared (FT-IR) spectra of purified poly-mannose and D-mannose were recorded on a Nicolet 560 spectrometer (Nicolet Co., USA). Both samples were blended with solid potassium bromide (KBr) powder at the same dosage, and the blend was made into a pellet. The KBr pellet was subjected to FTIR spectrophotometry and recorded at the transmittance mode from 4000 cm^{-1} to 400 cm^{-1}.

2.8. Methylation analysis

The methylation analysis of poly-mannose was conducted according to the method of Hakomori (1964). Dry samples (20 mg) were dissolved in 6 mL DMSO by incubating it at room temperature for 2 h. Aliquots of methylsulphenyl anion were added while argon was sparging at room temperature for 2 h until the color faded. The mixture was then transferred to ice bath, 4 mL methylation agent CH_3I was carefully pipetted and the mixture was incubated for 3 h. Finally water was added to terminate the reaction. The mixture was dialyzed for 24 h and dried under a stream of argon gas. The methylated product was then hydrolyzed with formic acid (1 mL) at 100 °C

for 1 h. After formic acid was removed, 2 mL 4 M trifluoroacetic acid (TFA) was added to the sample in an ampoule bottle, sparged with argon gas, sealed, and heated at 100 °C for 6 h. The mixture was then cooled, and dried under a stream of argon gas. The sample was then dissolved in 0.6 mL distilled water, reduced with sodium borohydride, acetylated with (1:1) pyridine–acetic anhydride at 100 °C for 2 h. Aliquots of the resultant partially methylated alditol acetates (PMAA) were injected into a GC–MS system (Agilent, USA) fitted with a TR-35MS column (30 m × 0.25 mm × 0.25 mm, 80–200 °C at 15 °C/min, then 200–260 °C at 10 °C/min) and an iron-trap MS detector.

2.9. ^{1}H, ^{13}C and 2D NMR spectroscopy

The poly-mannose was dissolved in 4 mL of D_2O at 70 °C with stirring for 2 h and freeze dried. This process was repeated three times. The sample was then dissolved in 3 mL of D_2O. High-resolution ^{1}H and ^{13}C NMR spectra were recorded at 500.13 and 125.77 MHz, respectively, on a Bruker DRX-500 spectrometer operating at a sample temperature of 25 °C. A 5-mm inverse geometry $^{1}H/^{13}C/^{15}N$ probe was used. Homonuclear ^{1}H–^{1}H correlation spectroscopy (COSY, TOCSY) and heteronuclear ^{1}H–^{13}C correlation experiments (HMQC, HMBC) were run using the standard Bruker (Bruker, Germany) pulse sequence.

3. Results and discussion

3.1. Effect of temperature, time, and proton on poly-mannose synthesis

Poly-mannose was synthesized using D-mannose as reactant, phosphoric acid as catalyst via an improved route assisted by microwave irradiation. The effects of reaction temperature, reaction time, and proton concentration on the yield of poly-mannose are listed as follows:

Temperature plays pivotal roles in poly-mannose synthesis rate and yield ratio. In this study, the optimum temperature for poly-mannose synthesis was shown to be 115 °C (Fig. 2a), under the condition of constant microwave power output of 900 W, reaction time 5 min, and proton concentration 2.5 mol/L.

Reaction time is one of the important factors for efficient synthesis. Therefore, time course studies on poly-mannose synthesis were performed for 5 min (Fig. 2b) with temperature of 115 °C and proton concentration 2.5 mol/L. The maximum poly-mannose yield rate was 91.46% after 5 min of microwave irradiation.

Phosphoric acid was used as catalyst to accelerate the polymerization of D-mannose. As shown (Fig. 2c), the poly-mannose yield rate improved with increasing concentration of proton until they reached the peak value of approximately 2.5 mol/L. The other optimal conditions were the reaction temperature of 115 °C and reaction time 5 min.

3.2. Monosaccharide identification and molecular weight analyses of poly-mannose

The ethanol-precipitated poly-mannose was hydrolyzed using 2 mol/L TFA for 4.5 h, and then the hydrolysate was detected by HPAEC. As shown in Table 1, the composition of ethanol precipitated poly-mannose was D-mannose and trace D-glucose.

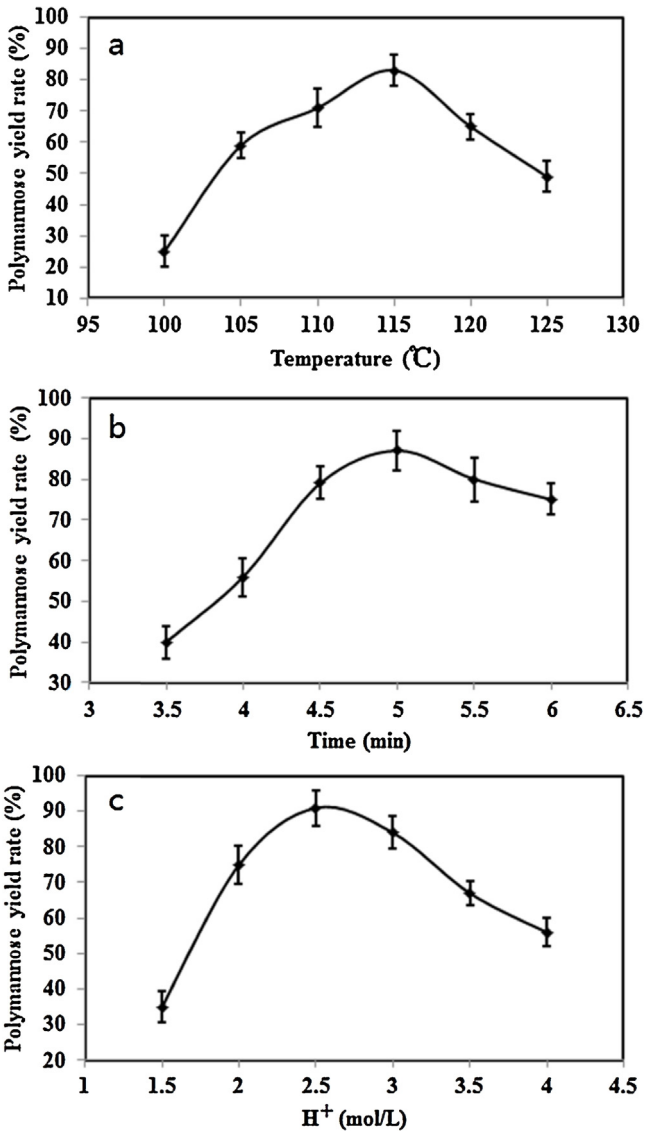

Fig. 2. Effect of temperature (a), time (b), and proton (c) on poly-mannose synthesis.

Purified poly-mannose was eluted as a single symmetrical sharp peak on HPGPC and the molecular weight distribution coefficient (Mw/Mn) 1.16 indicated that purified poly-mannose was homogeneous. The weight average molecular weight (Mw) was calculated to be 2.457 kDa, the number average molecular weight (Mn) was 2.105 kDa, and the average degree of polymerization (DP) was about 15.

Table 1
Monosaccharide composition and molecular weight of polysaccharides.

Polysaccharides	Composition of polysaccharide (%)			Molecular weight (kDa)[b]		
	D-glucose	D-galactose	D-mannose	Mw	Mn	Mw/Mn
Poly-mannose	0.19	–[a]	99.81	2.457	2.105	1.16

[a] Not detectable.
[b] Molecular weight determination of poly-mannose containing weight average molecular weight (Mw) and number average molecular weight (Mn).

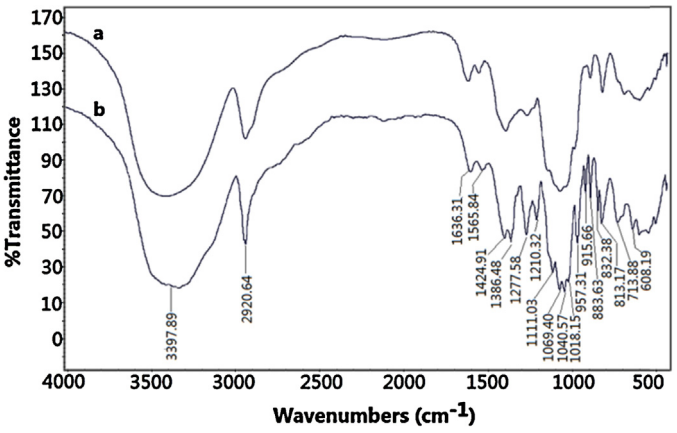

Fig. 3. Fourier transform infrared spectra of poly-mannose (a) and D-mannose (b).

3.3. FT-IR spectra analysis of poly-mannose

The FT-IR spectrum of poly-mannose and D-mannose is presented in Fig. 3. The attributions of the main absorptions were characteristic of glycosidic structures and were related to C—O stretching (1410.68 cm^{-1}) and anomeric C1—H group vibration (880.23 cm^{-1}). The spectral shape (Fig. 3a) with diminished bands at about 608.19 cm^{-1}, 832.38 cm^{-1}, 915.66 cm^{-1}, 957.31 cm^{-1}, and 1210.32 cm^{-1} was ascribed to the polymerization of D-mannose, which indicated that the condensation reaction of D-mannose occurred at the condition of acid catalyzed. Moreover, the marker bands at 813.17 cm^{-1} and 1069.40 cm^{-1} in the IR spectra were the characteristic absorptions of D-mannose. The absorption bands at 832.38 cm^{-1} and 880.23 cm^{-1} indicated the α- and β-configurations existing in polysaccharides (Zhang, Liu, Xiao, Zhang, & Sun, 2014). The region below 1200 cm^{-1} has previously been suggested as promising for analysis of structural conversions, the absorption bands at 1000–1200 cm^{-1} were due to C—O—C stretching vibration (Vieira et al., 2013). The small peaks at 1638.05 cm^{-1} and 1573.14 cm^{-1} resulted from —C=O stretching and —C—O stretching, respectively (Feng, Li, & Wang, 2010). Further analysis of the FT-IR spectra revealed that the broader band of absorption between 3700 cm^{-1} and 3000 cm^{-1} was due to O—H stretching. The absorption at 3403.91 cm^{-1} is attributed to the hydroxyl (—OH) stretching vibration and the band at 2928.64 cm^{-1} is due to C—H stretching vibration (Liu et al., 2007). These results indicated that poly-mannose was synthesized by phosphoric acid catalyzation under microwave irradiation.

3.4. Methylation analysis

Further detailed structural information was investigated using methylation analysis for poly-mannose (Table 2). The molar ratio of the sugar residues 3-Man*p* and 3,6-Man*p* were higher than 20%, thus these residues were the main building blocks of the polysaccharide chain. In addition, 6-Man*p* was detected with a comparable percentage. Sugar residues 2-Man*p*, 4-Man*p* and 2,4-Man*p* were also observed in poly-mannose, but were only of a small percentage of the total sugars. Based on the above results, we inferred that the backbone consisting of (1 → 3)-linked, and (1 → 6)-linked mannopyranose residues, and the main chain were branched at the O-2, O-3, O-4, O-6 position.

3.5. 1D and 2D NMR spectroscopy

1D and 2D NMR spectra were employed to confirm the structural deductions and provide more detailed structural information. The ^{1}H NMR spectrum of the poly-mannose at 25 °C is shown in Fig. 4a. The peaks in the anomeric region are assigned as 4.74, 4.93, 5.05, 5.15, 5.19, and 5.25 ppm. In the ^{13}C NMR spectrum, six anomeric carbon signals appeared at 110.1, 104.8, 104.1, 103.2, 102.1, and 96.9 ppm (Fig. 4b). All the ^{1}H and ^{13}C signals were assigned using COSY (Fig. 5a), TOCSY (Fig. 5b), HMQC (Fig. 6a), and HMBC (Fig. 6b).

The ^{1}H assignments were achieved through the COSY spectrum (Fig. 5a). Taking the anomeric proton $\delta_{H\text{-}1}$ = 4.93 ppm as an example, the COSY correlations between H-1 and H-2, H-2 and H-3, H-3 and H-4, H-4 and H-5, and H-5 and H-6/H-6′ (Fig. 5a) assigned the proton chemical shifts (Table 3). Based on the data from the HMQC spectrum (Fig. 6a), the corresponding ^{13}C assignments from C-1 to C-6 were also achieved as 102.1, 68.0, 73.0, 63.4, 75.2, and 68.2 ppm. The HMBC spectrum (Fig. 6b) analysis showed that, when the chemical shift of H-1 at 4.93 ppm, the correlations arising from $^{3}J_{H,C,C}$ and $^{3}J_{H,O,C}$ were obtained, and the chemical shifts of C-3 and C-5 were assigned as 73.0 and 73.5 ppm, respectively. From the HMQC spectrum (Fig. 6a), the corresponding ^{1}H assignments of H-3 and H-5 were achieved as 3.93 and 3.81 ppm, which were consistent with the COSY spectrum results. These results were further confirmed by the TOCSY spectrum where several well-resolved cross peaks at 4.93, 402, 3.97, 3.89, and 3.87 ppm (along the line start from 4.93 ppm) were detected (Fig. 5b). All the assignments of ^{1}H and ^{13}C resonances are summarized in Table 3.

The two vicinal (H-1 and H-2) protons of mannopyranose residues have no or small couplings (Cui, 2005; Ghosh et al., 2008), which prevent the detection of cross peaks and therefore, the J-network cannot be established, as shown in Fig. 5a, there are few signals in anomeric protons region between 4.3 and 5.8 ppm. However, the HMQC correlations (Fig. 6a) and HMBC correlations (Fig. 6b) can provide much more information about the anomeric protons and nonanomeric protons; it allows a one-to-one match of the ^{13}C and ^{1}H resonances. Chemical structure analysis of D-mannose shows that C-6 is an oxygenated methylene. Thus the HMQC correlations assigned the chemical shifts of H-6/H-6′ at 3.81/3.90, 3.69/3.83, 3.83/3.97, and 3.87/3.99 ppm (Fig. 6a). Taking the chemical shift of H-6/H-6′ at 3.87/3.99 ppm as an example, information to C-4 of the mannopyranose residues was obtained from analysis of the long-range heteronuclear correlation spectrum (HMBC) (Fig. 6b), the chemical shifts are assigned as $\delta_{C\text{-}4}$ = 75.4 ppm and $\delta_{H\text{-}2}$ = 3.42 ppm. From HMQC spectrum (Fig. 6a), the H-4 and C-2 chemical shifts are assigned as 3.78 and 78.9 ppm, respectively. The COSY spectrum (Fig. 5a) assigned the chemical shifts of the

Table 2
Sugar linkage analysis of poly-mannose.

Sugar derivative	Mode of linkage	mol%	Mass fragments
2,3,4,6-O-Me_4-Man*p*[a]	Man*p*-(1→	5.0	43,45,87,101,117,129,145,161,205
3,4,6-O-Me_3-Man*p*	→2)-Man*p*-(1→	0.3	43,45,71,74,87,99,101,129,161,189
2,4,6-O-Me_3-Man*p*	→3)-Man*p*-(1→	43.1	43,45,59,87,118,128,161,234,277
2,3,6-O-Me_3-Man*p*	→4)-Man*p*-(1→	1.6	45,87,101,113,117,61,233
2,3,4-O-Me_3-Man*p*	→6)-Man*p*-(1→	18.2	43,87,99,101,113,117,129,161,173,189
2,4-O-Me_2-Man*p*	→3,6)-Man*p*-(1→	24.5	41,43,45,71,87,99,101,117,129,189
3,6-O-Me_2-Man*p*	→2,4)-Man*p*-(1→	0.8	43,45,71,87,99,113,117,129,189,233

[a] 2,3,4,6-O-Me_4-Man*p* = 1,5-anhydro-2,3,4,6-tetra-O-methylmannitol, etc.

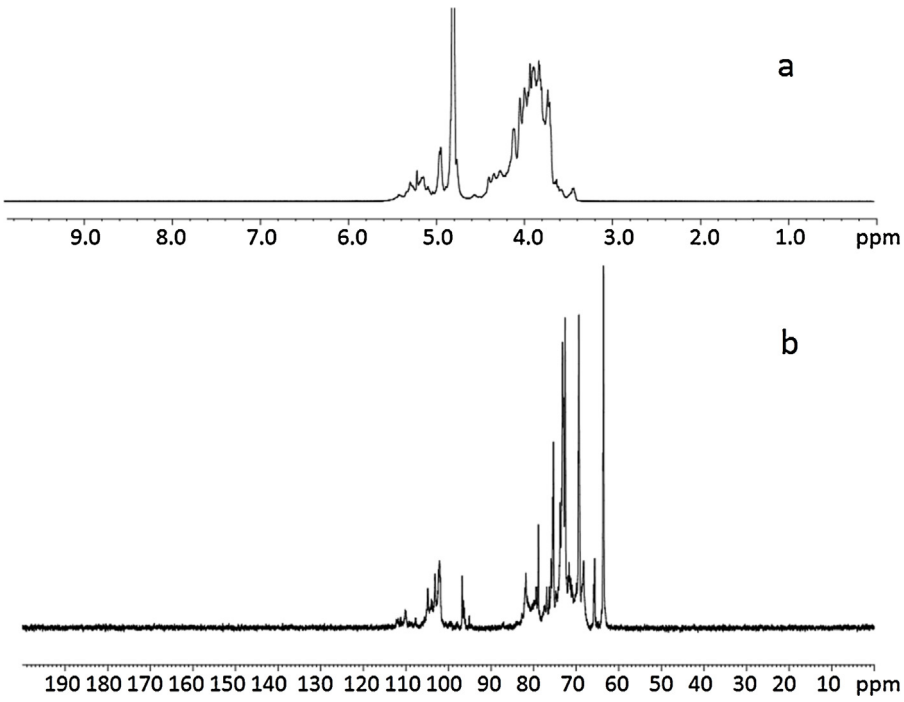

Fig. 4. ^{1}H NMR spectrum (a) (500 MHz, D_2O, 25 °C) and ^{13}C NMR spectrum (b) (125 MHz, D_2O, 25 °C) of poly-mannose.

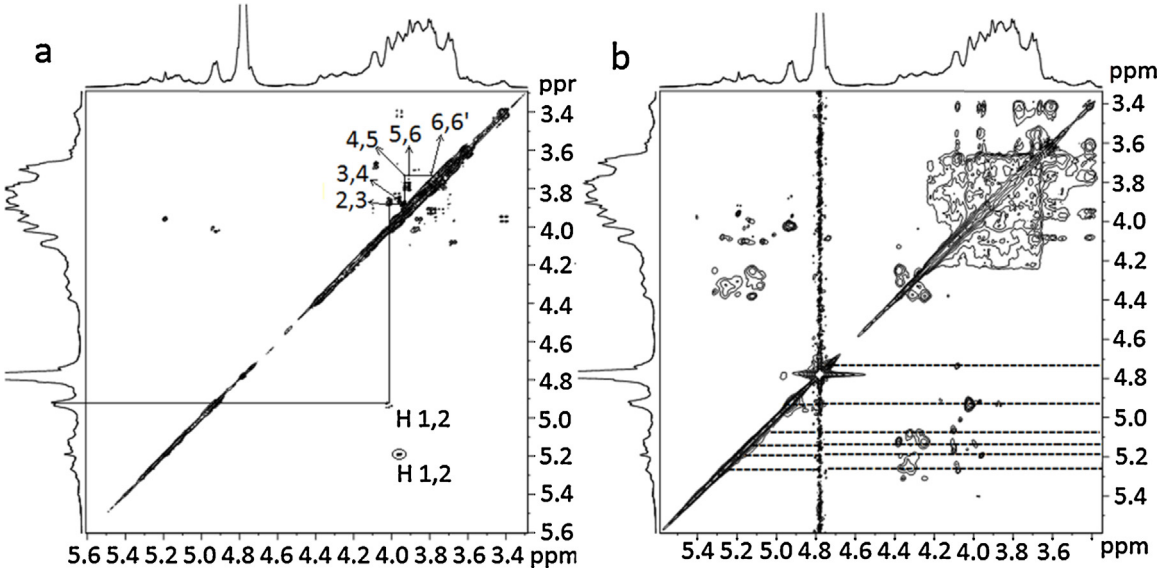

Fig. 5. COSY spectrum (a) and TOCSY spectrum (b) (25 °C in D_2O) of poly-mannose. (The full assignment of mannosyl residue was shown and the H1,2 cross peaks of the rest of the sugar residues are marked in the circle.)

Table 3
^{1}H and ^{13}C chemical shifts of poly-mannose based on homonuclear correlation (^{1}H–^{1}H COSY and TOCSY (Fig.5)), and heteronuclear correlation (^{1}H–^{13}C HMQC and ^{1}H–^{13}C HMBC (Fig.6)).

Mannosyl residue	Chemical shift δ (ppm)						
	H1/C1	H2/C2	H3/C3	H4/C4	H5/C5	H6/C6	H6′
O-3 substituted	4.74/103.0	4.11/70.5	3.89/73.0	3.95/63.4	3.42/78.8	3.55/76.8	3.78
	5.08/104.6	3.69/75.2	4.09.72.9	3.92/63.4	–/–[a]	–/–	–/–
	5.15/104.8	3.79/75.8	3.89/73.0	3.61/69.5	–/–	–/–	–
	5.19/96.6	3.97/71.5	3.87/73.0	–/–	–/–	–/–	–
O-6 substituted	–/–	3.42/78.9	3.97/71.5	3.78/75.4	–/–	3.87/73.0	3.99
	–/–	3.71/69.5	3.97/71.5	3.76/63.5	–/–	3.83/68.2	3.97
O-3,6 substituted	4.93/102.1	4.02/68.0	3.89/73.0	3.93/63.4	3.72/75.2	3.81/68.2	3.87

[a] Not obtained.

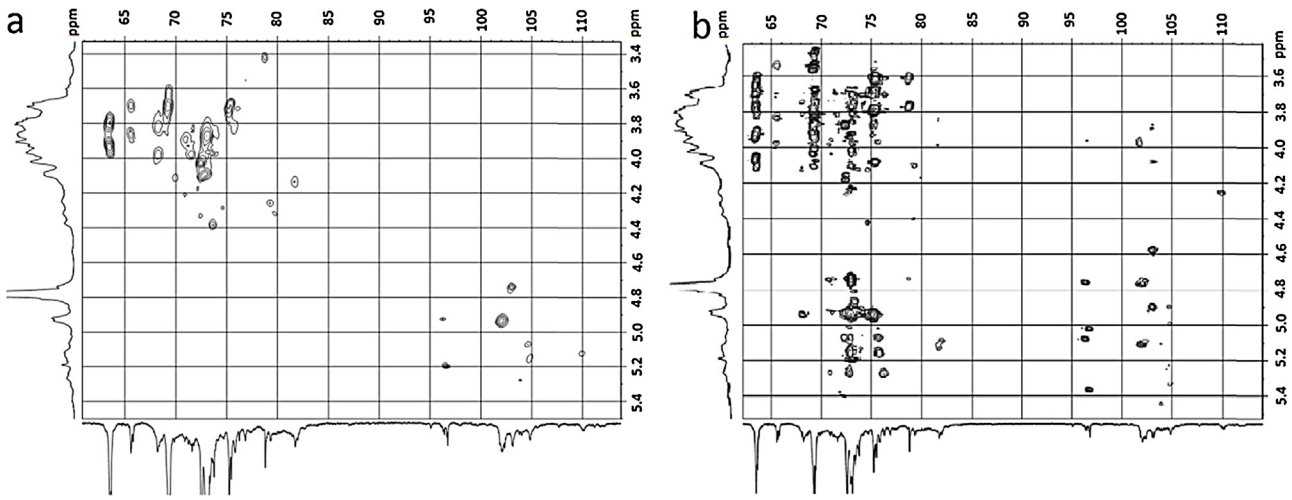

Fig. 6. HMQC spectrum (a) and HMBC spectrum (b) of poly-mannose (25 °C in D_2O).

$\delta_{H\text{-}3}$ = 3.97 ppm and, from HMQC spectrum (Fig. 6a), the C-3 was assigned as $\delta_{c\text{-}3}$ = 73.1 ppm. These results were also confirmed by the COSY spectrum (Fig. 5a) and TOCSY spectrum (Fig. 5b).

The long-range correlation (HMBC) spectra (Fig. 6b) showed that when the resonances of carbon signal at 68.2 ppm, the correlated resonance of hydrogen signal will appear at 4.93 ppm. Similarly, when the carbon resonance appears at 73 ppm, the correlated hydrogen resonance will appear at 4.74, 4.93, 5.08, 5.15, 5.19, and 5.26 ppm, respectively. Therefore, the H-1/C-1 signal at 4.74/103.0 ppm indicated that the residues should be assigned to (1 → 3)-linked β-D-mannopyranosyl (Patra et al., 2013; Prestegard, Miner, & Tyrell, 1983). However, the anomeric chemical shifts of H-1/C-1 at 5.08/104.6, 5.15/104.8, and 5.19/96.6 ppm should be assigned to (1 → 3)-linked α-D-mannopyranose residues (Cui, 2005; Ližičárová, Matulová, Machová, & Capek, 2007; Takahashi, Kudoh, Okawa, & Shibata, 2012). The signal of anomeric chemical shift of H-1/C-1 at 4.93/102.1 ppm corresponded to (1 → 3,6)-linked α-D-mannopyranose residues (Liu et al., 2013; Patra et al., 2013). The H-6/H-6′ signals at 3.83/3.97 and 3.87/3.99 ppm indicated that the residues could be assigned to (1 → 6)-linked α-D-mannopyranose residues (Yan et al., 2014). The NMR spectroscopy analyses did not obtain the linkage information of (1 → 2)-linked, (1 → 4)-linked, (1 → 2,4)-linked D-mannopyranose residues, whereas they were observed in methylation analysis (Table 2). This inconsistency might result from the small percentage of these linkages of sugar residues.

4. Conclusions

In this study, poly-mannose was synthesized using phosphoric acid as catalyst and microwave irradiation as a principal energy source for the first time. The optimum conditions were microwave output power 900 W, reaction temperature 115 °C, proton concentration 2.5 mol/L, and microwave irradiation time 5 min. The actual maximum yield was 91.46%.

Additionally the synthesized product was purified and characterized by HPAEC, HPGPC, FT-IR spectrum, methylation analysis, and NMR spectroscopy. HPAEC and HPGPC analysis showed that the monosaccharide composition of synthetic polysaccharides was D-mannose and the average degree of polymerization (DP) was about 15. FI-IR spectrum indicated the polymerization of D-mannose catalyzed by acid under the condition of microwave irradiation. Methylation analysis and NMR spectroscopy results suggested that both α- and β-anomeric configurations are existing in poly-mannose, the backbone consisting of (1 → 3)-linked β-D-Man*p*, (1 → 3)-linked α-D-Man*p*, and (1 → 6)-linked α-D-Man*p* residues, and the main chain were branched at the O-2, O-3, O-4, O-6 position.

Acknowledgment

The authors are grateful for the financial support from the 12th Five-Year Plan for Science and Technology Development of China (No. 2012BAD33B05) and Natural Science Foundation of Jiangsu Province (No. BK20140147) for this work.

References

Allingham, R. P. (1982). Polydextrose-a new food ingredient: Technical aspects. In G. Charalambous (Ed.), *Chemistry of foods and beverages: Recent developments* (pp. 293–303). New York: Academic Press Inc.

Cerna, M., Barros, A. S., Nunes, A., Rocha, S. M., Delgadillo, I., Copikova, J., et al. (2003). Use of FT-IR spectroscopy as a tool for the analysis of polysaccharide food additives. *Carbohydrate Polymers*, *51*, 383–389.

Cui, S. W. (2005). *Food carbohydrates: Chemistry, physical properties and applications*. Boca Raton, FL: Taylor & Francis Group: CRC Press (Chapter 1 and Chapter 3).

Feng, H., Li, J., & Wang, L. (2010). Preparation of biodegradable flax shive cellulose-based superabsorbent polymer under microwave irradiation. *BioResources*, *5*(3), 1484–1495.

Ghosh, K., Chandra, K., Roy, S. K., Mondal, S., Maiti, D., Das, D., et al. (2008). Structural investigation of a polysaccharide (Fr. I) isolated from the aqueous extract of an edible mushroom, *Volvariella diplasia*. *Carbohydrate Research*, *343*(2008), 1071–1078.

Hakomori, S. (1964). A rapid permethylation of glycolipid, and polysaccharide catalyzed by methylsulfinyl carbanion in dimethylsulfoxide. *Biochemistry*, *55*(2), 205–208.

Jiang, G., Wen, L., Chen, F., Wu, F., Lin, S., Yang, B., et al. (2013). Structural characteristics and antioxidant activities of polysaccharides from longan seed. *Carbohydrate Polymers*, *92*, 758–764.

Križková, L., Žitňanová, I., Mislovičová, D., Masárová, J., Sasinková, V., Ďuračková, Z., et al. (2006). Antioxidant and antimutagenic activity of mannan neoglycoconjugates: Mannan-human serum albumin and mannan-penicillin G acylase. *Genetic Toxicology and Environmental Mutagenesis*, *606*, 72–79.

Lewis, J. E., McDaniel, H. R., Agronin, M. E., Loewenstein, D. A., Riveros, J., Mestre, R., et al. (2013). The effect of an aloe polymannose multinutrient complex on cognitive and immune functioning in Alzheimer's disease. *Journal of Alzheimers Disease*, *33*.

Li, X. M., Le, G. W., & Shi, Y. H. (2006). Microwave-assisted solid-phase oligosaccharides synthesis reaction and scavenging activity of synthetic product to free radical. *Carbohydrate Polymers*, *64*(2), 274–281.

Li, X. M., Le, G. W., Cheng, J. X., Wang, F., & Shi, Y. H. (2006). Optimization of microwave-assisted solid-phase oligosaccharides synthesis reaction and analysis of components and structure of synthetic product. *Carbohydrate Polymers*, *64*(2), 408–418.

Li, X., Liu, F., Li, Z., Ye, N., Huang, C., & Yuan, X. (2014). *Atractylodes macrocephala* polysaccharides induces mitochondrial-mediated apoptosis in glioma C6 cells. *International Journal of Biological Macromolecules*, *66*, 108–112.

Liu, C., Lin, Q., Gao, Y., Ye, L., Xing, Y., & Xi, T. (2007). Characterization and antitumor activity of a polysaccharide from *Strongylocentrotus nudus* eggs. *Carbohydrate Polymers*, *67*, 313–318.

Liu, D., Liao, N. B., Ye, X. Q., Hu, Y. Q., Wu, D., Guo, X., et al. (2013). Isolation and structural characterization of a novel antioxidant mannoglucan from a marine bubble snail, *Bullacta exarata* (Philippi). *Marine Drugs*, *11*, 4464–4477.

Ližičárová, I., Matulová, M., Machová, E., & Capek, P. (2007). Cell wall mannan of human pathogen *Candida dublinienisis*. *Carbohydrate Polymers*, *68*(2007), 191–195.

Manley-Harris, M., & Richards, G. N. (1993). A novel fructoglucan from the thermal polymerization of sucrose. *Carbohydrate Research*, *240*, 183–196.

MíčKoVá, K., čopíKoVá, J., & SyNytSyA, A. (2007). Determination of polydextrose as a fat replacer in butter. *Czech Journal of Food Science*, *25*, 25–31.

Patra, S., Patra, P., Maity, K. K., Mandal, S., Bhunia, S. K., Dey, B., et al. (2013). A heteroglycan from the mycelia of *Pleurotus ostreatus*: Structure determination and study of antioxidant properties. *Carbohydrate Research*, *368*(2013), 16–21.

Prestegard, J. H., Miner, V. W., & Tyrell, P. M. (1983). Deuterium NMR as a structural probe for micelle-associated carbohydrates: D-mannose. *Proceedings of the National Academy of Sciences of the United States of America*, *80*, 7192–7196.

Qu, H. M., Liu, S. J., & Zhang, C. Y. (2014). Antitumor and antiangiogenic activity of *Schisandra chinensis* polysaccharide in a renal cell carcinoma model. *International Journal of Biological Macromolecules*, *66*, 52–56.

Takahashi, S., Kudoh, A., Okawa, Y., & Shibata, N. (2012). Significant differences in the cell-wall mannans from three *Candida glabrata* strains correlate with antifungal drug sensitivity. *The FEBS Journal*, *279*(2012), 1844–1856.

Vieira, A. C., Serra, A. C., Carvalho, R. A., Gonsalves, A., Figueiras, A., Veiga, F. J., et al. (2013). Microwave synthesis and in vitro stability of diclofenac-β-cyclodextrin conjugate for colon delivery. *Carbohydrate Polymers*, *93*, 512–517.

Vu, B., Chen, M., Crawford, R. J., & Ivanova, E. P. (2009). Bacterial extracellular polysaccharides involved in biofilm formation. *Molecules*, *14*, 2535–2554.

Wang, H., Liu, G., Zhou, B., & Hu, X. (2012). Monosaccharide compositional analysis of purified polysaccharide from *Tricholoma matsutake* by capillary gas chromatography. *Journal of Medicinal Plants Research*, *6*(10), 1935–1940.

Wang, H., Shi, Y., & Le, G. (2014). Rapid microwave-assisted synthesis of polydextrose and identification of structure and function. *Carbohydrate Polymers*, *113*, 225–230.

Yan, M. X., Mao, W. J., Chen, C. L., Kong, X. L., Gu, Q. Q., Li, N., et al. (2014). Structural elucidation of the exopolysaccharide produced by the mangrove fungus *Penicillium solitum*. *Carbohydrate Polymers*, *111*(2014), 485–491.

Zhang, A., Liu, Y., Xiao, N., Zhang, Y., & Sun, P. (2014). Structural investigation of a novel heteropolysaccharide from the fruiting bodies of *Boletus edulis*. *Food Chemistry*, *146*(1), 334–338.

Zia, K. M., Anjum, S., Zuber, M., Mujahid, M., & Jamil, T. (2014). Synthesis and molecular characterization of chitosan based polyurethane elastomers using aromatic diisocyanate. *International Journal of Biological Macromolecules*, *66*, 26–32.